JCTC Journal of Chemical Theory and Computation

Article

pubs.acs.org/JCTC

Linearized Coupled Cluster Correction on the Antisymmetric Product of 1-Reference Orbital Geminals

Katharina Boguslawski*,† and Paul W. Ayers‡

†Institute of Physics, Faculty of Physics, Astronomy and Informatics, Nicolaus Copernicus University, Grudziadzka 5, 87-100 Torun, Poland

‡Department of Chemistry and Chemical Biology, McMaster University, 1280 Main Street West, Hamilton, ON, L8S 4M1, Canada

Supporting Information

ABSTRACT: We present a linearized coupled cluster (LCC) correction based on a reference state of the antisymmetric product of 1-reference orbital geminals (AP1roG). In our LCC ansatz, the cluster operator is restricted to double or to single and double excitations, as in standard single-reference CC theory. The performance of the AP1roG-LCC models is tested for the dissociation of diatomic molecules in their lowest-lying singlet state (C_2, F_2, and BN), the symmetric dissociation of the H_{50} hydrogen chain, and spectroscopic constants of the uranyl cation (UO_2^{2+}). Our study indicates that an LCC correction based on an AP1roG reference function is more robust and reliable than corrections based on perturbation theory, yielding spectroscopic constants that are in very good agreement with theoretical reference data.

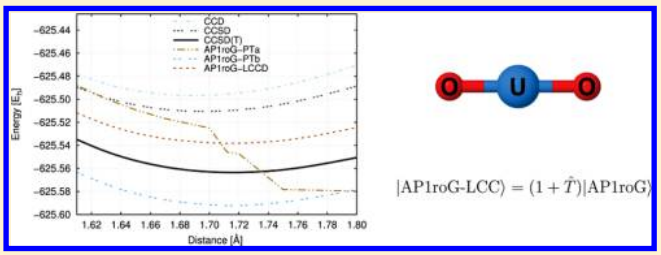

1. INTRODUCTION

Unlike quantum-chemistry methods for modeling small- and medium-sized molecules,[1,2] routine applications to larger molecular systems are hampered because conventional methods are either too expensive or too approximate to guarantee reliable results. These problems are particularly severe for molecules with strong electron correlation. Examples of strongly correlated systems are radicals, transition metals, and actinide compounds. Furthermore, well-established approaches for strong correlation scale poorly, often factorially, with system size. These drawbacks motivate the development of new, low-cost electron correlation methods for strongly correlated many-body systems.

One active field of research for strongly correlated systems focuses on the development of wave function methods that use two-electron functions (geminals) to model the correlated motion of electrons.[3−7] The most popular geminal-based approaches are the antisymmetric product of strongly orthogonal geminals[3,8−14] (APSG), the antisymmetrized geminal power[15−18] (which is a special case of projected Hartree−Fock−Bogoliubov[19]), the antisymmetric product of interacting geminals[4,20−31] (APIG), generalized valence bond[8,32−35] (GVB), and the antisymmetric product of 1-reference orbital geminals (AP1roG).[36−38] Specifically, AP1roG provides a very good approximation to the doubly occupied configuration interaction[39] (DOCI) wave function, and it does so at mean-field computational cost. The AP1roG geminal creation operator reads

$$\phi_i^\dagger = a_i^\dagger a_{\bar{i}}^\dagger + \sum_a c_i^a a_a^\dagger a_{\bar{a}}^\dagger \tag{1}$$

where $a_p^\dagger$ and $a_{\bar{p}}^\dagger$ are the standard Fermionic creation operators for spin-up (p) and spin-down electrons ($\bar{p}$), c_i^a are the geminal coefficients, and the summation runs over all virtual orbitals. Specifically, the AP1roG geminal coefficient matrix has the form

$$\mathbf{c}_{\mathrm{AP1roG}} = \begin{pmatrix} 1 & \cdots & 0 & 0 & c_1^{P+1} & c_1^{P+2} & \cdots & c_1^K \\ 0 & 1 & \cdots & 0 & c_2^{P+1} & c_2^{P+2} & \cdots & c_2^K \\ \vdots & \vdots & \ddots & & \vdots & \vdots & \ddots & \vdots \\ 0 & \vdots & \cdots & 1 & c_P^{P+1} & c_P^{P+2} & \cdots & c_P^K \end{pmatrix} \tag{2}$$

where K denotes the number of basis functions, P is the number of electron pairs, and the left sub-block of $\mathbf{c}_{\mathrm{AP1roG}}$ encodes some reference determinant. The geminal matrix connects each geminal with the underlying one-particle basis functions. We should note that if we impose specific restrictions on the structure of the above matrix then we can deduce different geminal models in the APIG family.[5]

The electronic wave function is written as a product of geminal creation operators for all electron pairs P acting on the vacuum state, $|\mathrm{AP1roG}\rangle = \prod_i^P \phi_i^\dagger|\rangle$. Unique among geminal methods, the AP1roG wave function ansatz can be rewritten in terms of one-particle functions as a fully general pair-coupled-cluster-doubles[40] (pCCD) wave function

Received: August 12, 2015
Published: October 14, 2015

DOI: 10.1021/acs.jctc.5b00776
J. Chem. Theory Comput. 2015, 11, 5252−5261

$$|\mathrm{AP1roG}\rangle = \exp\left(\sum_{i=1}^{P}\sum_{a=P+1}^{K} c_i^a a_a^\dagger a_{\bar{a}}^\dagger a_{\bar{i}} a_i\right)|\Phi_0\rangle \tag{3}$$

where $|\Phi_0\rangle$ is some independent-particle wave function (for instance, the Hartree−Fock (HF) determinant). The exponential ansatz of AP1roG (cf. eq 3) ensures the size-extensivity of the model. However, to recover size-consistency, we have to optimize the one-particle basis functions. This can be done in a fully variational manner,[37,38] analogous to orbital-optimized coupled cluster,[41] using nonvariational orbital optimization techniques[42,43] or a stochastic random-walk algorithm.[44] A number of numerical studies on systems with strongly correlated electrons have shown the superiority of the variational orbital optimization procedure over the latter ones.[43] We should note that due to the four-index transformation of the electron repulsion integrals the computational scaling of the orbital-optimized AP1roG model deteriorates to $O(K^5)$.[37] Although restricted orbital-optimized AP1roG is limited to close-shell systems, it has already proven to be a reliable method for modeling strong electron correlation effects in quasi-degenerate systems,[37,42,43] single and multiple bond-breaking processes,[45,46] and actinide chemistry.[47]

As with all other geminal models, AP1roG misses a large fraction of weak (dynamical) electron correlation effects. To address this problem and account for weak electron correlation effects in the geminal reference wave function, various *a posteriori* corrections have been proposed. These include models based on single- and multireference perturbation theory,[31,48−51] extended random-phase approximation,[52−54] (linearized) coupled cluster theory,[35,55] and density functional theory.[54,56,57] In the case of AP1roG, dynamical correlation was included using perturbation theory,[49] single-reference coupled-cluster theory,[58] and density functional theory.[56,57] Recent studies on diatomic molecules, however, point out numerical instabilities and failures of the proposed perturbation theory corrections.[46] This motivates the pursuit of more robust dynamical correlation models for AP1roG. A reliable way to account for dynamical correlation effects *a posteriori* is to use a multireference linearized coupled cluster (LCC) correction. Recently, Zoboki et al. presented an LCC correction based on an APSG reference function and demonstrated the good performance of the APSG-MRLCC approach.[55] Their findings encouraged us to develop an LCC correction based on an AP1roG reference state.

This work is organized as follows. In Section 2, we will discuss two different LCC corrections for AP1roG. Their performance is compared by studying some well-known problems in quantum chemistry that require a balanced treatment of dynamical and strong electron correlation effects: the dissociation of the singlet ground state of C_2 and F_2, the dissociation of the first excited singlet state of BN, the symmetric dissociation of H_{50}, and the spectroscopic constants of the UO_2^{2+} molecule. Computational details are presented in Section 3, and numerical results are discussed in Section 4. Finally, we conclude in Section 5.

2. LCC THEORY WITH AN AP1ROG REFERENCE FUNCTION

In this work, dynamical correlation effects are built into the electronic wave function *a posteriori* using an exponential coupled cluster ansatz

$$|\Psi\rangle = \exp(\hat{T})|\mathrm{AP1roG}\rangle \tag{4}$$

where $\hat{T} = \sum_\nu t_\nu \hat{\tau}_\nu$ is a general cluster operator. The corresponding time-independent Schrödinger equation reads

$$\hat{H}\exp(\hat{T})|\mathrm{AP1roG}\rangle = E\exp(\hat{T})|\mathrm{AP1roG}\rangle \tag{5}$$

Multiplying from the left by $\exp(-\hat{T})$ and truncating the Baker−Campbell−Hausdorff expansion after the second term

$$\exp(-\hat{T})\hat{H}\exp(\hat{T}) \approx \hat{H} + [\hat{H},\hat{T}] \tag{6}$$

we arrive at the linearized coupled cluster Schrödinger equation

$$(\hat{H} + [\hat{H},\hat{T}])|\mathrm{AP1roG}\rangle = E|\mathrm{AP1roG}\rangle \tag{7}$$

To obtain the cluster amplitudes t_ν, we multiply from left by $\langle\nu|$

$$\langle\nu|(\hat{H} + [\hat{H},\hat{T}])|\mathrm{AP1roG}\rangle = 0 \tag{8}$$

where we assume that the excitation operator $\hat{\tau}_\nu$ creates states orthogonal to $|\mathrm{AP1roG}\rangle$, $\langle\nu|\mathrm{AP1roG}\rangle = 0$. The projection manifold $\{\nu\}$ will depend on the choice of the cluster operator $\hat{T}$ (vide infra).

The energy can be calculated by projecting against the reference determinant of $|\mathrm{AP1roG}\rangle$, i.e., multiplying eq 7 by $\langle\Phi_0|$ and using intermediate normalization

$$\langle\Phi_0|(\hat{H} + [\hat{H},\hat{T}])|\mathrm{AP1roG}\rangle = E \tag{9}$$

The only constraint on the cluster operator that we have made so far is that it creates states that are orthogonal to the AP1roG reference function. One suitable choice for the cluster operator is to include substitutions between the occupied and virtual orbitals with respect to $|\mathrm{AP1roG}\rangle$. If only double excitations are included, then the cluster operator is specified as

$$\hat{T}_2 = \frac{1}{2}\sum_{ij}^{\mathrm{occ}}\sum_{ab}^{\mathrm{virt}}{}' t_{ij}^{ab}\hat{E}_{ai}\hat{E}_{bj} \tag{10}$$

where $\hat{E}_{ai} = a_a^\dagger a_i + a_{\bar{a}}^\dagger a_{\bar{i}}$ is the singlet excitation operator and the cluster amplitudes are symmetric with respect to pair-exchange, i.e., $t_{ij}^{ab} = t_{ji}^{ba}$. The prime in the above summations indicates that pair-excited determinants are excluded in the cluster operator, i.e., $t_{i\bar{i}}^{a\bar{a}} = 0$ (as those excitations do not fulfill the orthogonality condition, $\langle\nu|\mathrm{AP1roG}\rangle = 0$).

To arrive at a computationally feasible model, we will further restrict the cluster operator of eq 10 to include only excitations with respect to the reference determinant, thereby excluding possible redundancies in excitations and amplitudes. The projection manifold then contains all doubly excited determinants with respect to $|\Phi_0\rangle$. Furthermore, as the basis for the bra states of the projection manifold, we will use the convenient choice[41]

$$\langle\overline{{}_{ij}^{ab}}| = \frac{1}{3}\langle{}_{ij}^{ab}| + \frac{1}{6}\langle{}_{ji}^{ab}| \tag{11}$$

where $\langle{}_{ij}^{ab}| = \langle\Phi_0|\hat{E}_{jb}\hat{E}_{ia}$. The bra basis then forms a biorthogonal basis that satisfies the normalization condition

$$\langle\overline{{}_{ij}^{ab}}|{}_{kl}^{cd}\rangle = \delta_{iajb,kcld} + \delta_{jbia,kcld} \tag{12}$$

The doubles amplitudes $\{t_{ij}^{ab}\}$ are obtained by solving a linear set of equations

$$B_\mu + \sum_\nu A_{\mu,\nu}t_\nu = 0 \tag{13}$$

DOI: 10.1021/acs.jctc.5b00776
J. Chem. Theory Comput. 2015, 11, 5252−5261

where the sum runs over all double excitations (without pair excitations) and $B_\mu = B_{iajb} = \langle \overline{ij}^{ab}|\hat{H}|\mathrm{AP1roG}\rangle$, whereas $A_{\mu,\nu} = A_{iajb,kcld} = \frac{1}{2}\langle \overline{ij}^{ab}|[\hat{H},\hat{E}_{ck}\hat{E}_{dl}]|\mathrm{AP1roG}\rangle$. The energy correction $E_{\mathrm{corr}}^{(D)}$ with respect to the AP1roG reference wave function is given as

$$E_{\mathrm{corr}}^{(D)} = \sum_{iajb} t_{ij}^{ab}(\langle ij||ab\rangle + \langle ij|ab\rangle) \tag{14}$$

where we have used the standard notation for the exchange integrals, $\langle ij||ab\rangle = \langle ij|ab\rangle - \langle ij|ba\rangle$, and physicists' notation for the two-electron integrals.

Similarly, the contribution of single excitations can be accounted for by including

$$\hat{T}_1 = \sum_{ia} t_i^a \hat{E}_{ai} \tag{15}$$

in the cluster operator. Restricting the single excitations to the AP1roG reference determinant $|\Phi_0\rangle$, the singles projection manifold contains all singly excited determinants with respect to $|\Phi_0\rangle$. In analogy to the doubles projection manifold, the bra states of the singles projection manifold are chosen to form a biorthogonal basis with the convenient normalization condition[41]

$$\langle \overline{i}^{a}|j^{b}\rangle = \delta_{ai,bj} \tag{16}$$

where $\langle \overline{i}^{a}| = \frac{1}{2}\langle i^a| = \frac{1}{2}\langle\Phi_0|\hat{E}_{ia}$. The single and double amplitudes are obtained by solving a coupled set of linear equations equivalent to eq 13, where μ and ν now run over all single and double excitations. The energy correction with respect to the AP1roG reference value is

$$E_{\mathrm{corr}}^{(S,D)} = 2\sum_{ia} F_{ia}t_i^a + \sum_{iajb} t_{ij}^{ab}(\langle ij||ab\rangle + \langle ij|ab\rangle) \tag{17}$$

where F_{ia} are the elements of the Fock matrix, $F_{ia} = h_{ia} + \sum_m^{\mathrm{occ}}(\langle am||im\rangle + \langle am|im\rangle)$, and h_{ia} are the one-electron integrals. Note that, in contrast to canonical Hartree−Fock orbitals, the Fock matrix is not diagonal when the orbitals are optimized within AP1roG. In the AP1roG-LCC approach, the single excitations thus contribute both directly to the energy correction and indirectly through coupling to the doubles equations.

We will abbreviate the LCC correction using $\hat{T} = \hat{T}_2$ as AP1roG-LCCD, whereas AP1roG-LCCSD indicates that the cluster operator contains single and double excitations, $\hat{T} = \hat{T}_1 + \hat{T}_2$.

Finally, we should note that the LCCD and LCCSD corrections as outlined above are similar, but not equivalent to, the frozen-pCCD (fpCCD) and fpCCSD approaches, respectively.[58] Specifically, in fpCC, the equations for the pair amplitudes are solved first, which, in our case, is equivalent to solving the AP1roG amplitude equations. Then, the usual CCD/CCSD equations are solved without allowing the pair amplitudes to change. In AP1roG-LCC, we first solve for the AP1roG amplitudes, which is equivalent to the first step of a fpCC calculation, followed by solving for the remaining cluster amplitudes. In contrast to fpCC, our cluster operator is linearized (cf., eq 7) and thus all higher-order terms are eliminated, while the reference wave function is $|\mathrm{AP1roG}\rangle$ (instead of a single Slater determinant as in fpCC). Choosing $|\mathrm{AP1roG}\rangle$ as a reference function results in additional terms in the amplitude equations beyond the standard single-reference LCC approach arising from coupling to pair-excited Slater determinants with respect to $|\Phi_0\rangle$. This coupling to pair-excited Slater determinants leads to additional terms in the LCC amplitude equations that are also included in the fpCC amplitude equations. Therefore, our LCC approach can be considered to be a simplification of the fpCC method. (Other modifications of conventional CC-type methods that are suitable for strong correlation have been presented recently.[59,60]) Specifically, the connection between our LCCD corrections and fpCC can also be understood by rewriting the corresponding linearized coupled cluster Schrödinger eq 7 using the exponential ansatz for AP1roG explicitly

$$\exp(-\hat{T}_{\mathrm{p}})(\hat{H} + [\hat{H},\hat{T}_{\mathrm{np}}])\exp(\hat{T}_{\mathrm{p}})|\Phi_0\rangle = E|\Phi_0\rangle \tag{18}$$

where $\hat{T}_{\mathrm{p}}$ is the AP1roG (seniority zero) cluster operator containing only pair excitations and $\hat{T}_{\mathrm{np}}$ is the seniority nonzero cluster operator of eq 10. Note that we have used the labels p (pair) and np (nonpair) to emphasize the connection to fpCC methods. The seniority nonzero cluster amplitudes can be obtained by projection against $\langle\nu|$

$$\langle\nu|\hat{H} + [\hat{H},\hat{T}_{\mathrm{np}}] + [[\hat{H},\hat{T}_{\mathrm{np}}],\hat{T}_{\mathrm{p}}]|\Phi_0\rangle = 0 \tag{19}$$

which further illustrates the coupling to pair-excited Slater determinants generated by $\hat{T}_{\mathrm{p}}$ (compared to single-reference linearized coupled cluster). The above equation can be compared to the amplitude equations of (fp-)CC approaches in, for instance, refs 41 and 61. Since the most expensive contributions in the amplitude equations are similar in both AP1roG-LCCD/LCCSD and fp-CCD/CCSD, the computational scaling of our LCC correction is as $O(o^2v^4)$, where o and v are the number of occupied and virtual orbitals, respectively.

3. COMPUTATIONAL DETAILS

3.1. AP1roG. All geminal calculations have been performed in the Horton 2.0.0 software package.[62] All restricted (variationally) orbital-optimized AP1roG calculations were allowed to freely relax without any spatial symmetry constraints, i.e., no point group symmetry was imposed. For all molecules, all orbitals were active. In the following, we will abbreviate (variationally) orbital-optimized AP1roG as AP1roG. We should note that AP1roG is a product of natural geminals. Thus, the one-electron-reduced density matrix is diagonal, and the (optimized) orbitals are natural orbitals. We will refer to the variationally optimized AP1roG orbitals as natural orbitals.

3.2. PTa and PTb. The PTa and PTb calculations were performed using the Horton 2.0.0 software package.[62] For all molecules, the optimized AP1roG natural orbitals were chosen as the orbital basis, and all electrons and orbitals have been included in the active space.

3.3. LCCD and LCCSD. The linearized coupled cluster models with double and single and double excitations have been implemented in a developer version of Horton 2.0.0.[62] The natural orbitals of AP1roG were chosen as the orbital basis for all molecules studied. Furthermore, all electrons and orbitals were correlated.

3.4. Coupled Cluster. The coupled cluster doubles (CCD), CC singles and doubles (CCSD), and CC singles, doubles, and perturbative triples (CCSD(T)) calculations have been carried out in the DALTON2013 software package.[63] In each case, all

DOI: 10.1021/acs.jctc.5b00776
J. Chem. Theory Comput. 2015, 11, 5252−5261

Table 1. Spectroscopic Constants for the Dissociation of the C_2, F_2, and BN Molecule for Different Quantum Chemistry Methods and Basis Sets[a]

	method	E_e [E_h]	r_e [Å]	D_e [$\frac{kcal}{mol}$]	ω_e [cm^{-1}]	E_e [E_h]	r_e [Å]	D_e [$\frac{kcal}{mol}$]	ω_e [cm^{-1}]
		aug-cc-pVDZ				aug-cc-pVTZ			
C_2	AP1roG	−75.55256	1.240(−0.033)	104.6(−15.7)	1943(+134)	−75.58569	1.227(−0.025)	132.9(−8.2)	1780(−56)
	AP1roG-PTa	−75.73784	1.273(+0.000)	152.7(+22.4)	1901(+93)	−75.80222	1.251(+0.001)	160.4(+19.3)	1889(+53)
	AP1roG-PTb	−75.70689	1.260(−0.013)	116.3(−14.0)	1863(+55)	−75.78350	1.235(−0.017)	127.2(−13.9)	1938(+102)
	AP1roG-LCCD	−75.73848	1.274(−0.001)	124.0(−6.3)	1960(+151)	−75.81125	1.240(−0.012)	139.3(−1.8)	1916(+80)
	AP1roG-LCCSD	−75.73882	1.266(−0.007)	127.6(−2.7)	1855(+46)	−75.81257	1.240(−0.012)	143.0(+1.9)	1926(+90)
	NEVPT2	−75.71751	1.259(−0.014)	135.0(+4.7)	1924(+117)	−75.78829	1.244(−0.008)	148.0(+6.9)	1886(+50)
	MRCI-SD[66]	−75.73221	1.273	130.3	1809	−75.78079	1.252	141.1	1836
F_2	AP1roG	−198.88134	1.521(+0.068)	12.8(−15.7)	886(+85)	−198.96762	1.467(+0.047)	16.2(−7.7)	703(−189)
	AP1roG-PTa	−199.14227	1.398(−0.055)	30.1(+1.6)	636(−165)	−199.32912	1.448(+0.028)	33.7(−0.2)	847(−45)
	AP1roG-PTb	−199.13392	1.473(+0.020)		832 (+31)	−199.31858	1.417(−0.003)		891(−1)
	AP1roG-LCCD	−199.15802	1.466(+0.013)	39.5(+11.0)	780(−21)	−199.34112	1.433(+0.013)	45.5(+11.6)	872(−20)
	AP1roG-LCCSD	−199.15885	1.462(+0.009)	40.1(+11.6)	793(−8)	−199.34235	1.431(+0.011)	46.7(+12.8)	883(−9)
	CCSD	−199.13428	1.426(−0.017)	57.3(+18.8)	917(+116)	−199.29382	1.396(−0.024)	69.2(+35.3)	1004(+12)
	CCSD(T)	−199.14777	1.450(−0.003)		841(+ 40)	−199.31364	1.419(−0.001)		911(+19)
	MRCI-SD[66]	−199.12245	1.453	28.5	801	−199.27607	1.420	33.9	892
		cc-pVDZ				cc-pVTZ			
BN	AP1roG	−79.03693	1.310(+0.012)	107.0(−41.6)	1432(−218)	−79.07582	1.304(+0.019)	114.3(−40.1)	1630(−52)
	AP1roG-PTa	−79.21062	1.303(+0.005)	173.2(+24.6)	1670(+19)	−79.28333	1.283(−0.002)	181.3(+26.9)	1751(+68)
	AP1roG-PTb	−79.17814	1.289(−0.009)		1702(+51)	−79.25960	1.273(−0.012)		1739(+57)
	AP1roG-LCCD	−79.20387	1.294(−0.004)	165.1(+16.5)	1685(+34)	−79.28205	1.277(−0.008)	174.1(+19.8)	1734(+52)
	AP1roG-LCCSD	−79.20986	1.293(−0.005)	169.0(+20.4)	1694(+43)	−79.28975	1.275(−0.010)	178.6(+24.2)	1749(+67)
	CCSD(T)[68]		1.285(−0.013)		1698(+47)		1.244(−0.008)		1732(+50)
	RMR CCSD(T)[68]		1.298(±0.000)		1640(−11)		1.284(−0.001)		1681(+1)
	MRCI-SD+Q[67]	−79.20682	1.298	148.6	1651	−79.26794	1.285	154.4	1682

[a]The differences are with respect to MRCI-SD reference data[66] for C_2 and F_2 and with respect to MRCI-SD+Q reference data[67] for BN. E_e, ground state energy at r_e.

electrons and orbitals were correlated, and no spatial symmetry was imposed.

3.5. Relativity and Basis Sets. For the C_2 and F_2 molecules, Dunning's aug-cc-pVDZ (C, F: (10s5p2d) → [4s3p2d]) and aug-cc-pVTZ (C, F: (11s6p3d2f) → [5s4p3d2f]) basis sets were used, whereas Dunning's cc-pVDZ (B, N: (9s4p1d) → [3s2p1d]) and cc-pVTZ (B, N: (10s5p2d1f) → [4s,3p,2d,1f]) basis sets were used for BN. The STO-6G basis set was utilized for the H atoms in H_{50} to allow for a comparison to DMRG reference data to be made.

For UO_2^{2+}, scalar relativistic effects were incorporated through relativistic effective core potentials (RECP). In all calculations, we have used a small core (SC) RECP (60 electrons in the core) with the following contraction scheme: (12s11p10d8f) → [8s7p6d4f]. For lighter elements (O), the cc-pVDZ basis set of Dunning was employed, (10s5p1d) → [4s3p1d].

3.6. Fitting Procedure. The potential energy curves of diatomic molecules were obtained by varying bond lengths in the range of 1.2−4.0 and 1.1−3.2 Å for F_2 and C_2 molecules, respectively, and in the range of 1.1−6.0 Å for the first excited state of the BN molecule. The points on the resulting potential energy curve were used for a subsequent generalized Morse function[64] fit to obtain the equilibrium bond lengths (R_e) and potential energy depths (D_e). The harmonic vibrational frequencies (ω_e) were calculated numerically using the five-point finite difference stencil.[65]

4. NUMERICAL RESULTS

4.1. Dissociation of C_2. The carbon dimer is one of the most complex diatomic molecules that can be formed from the first-row elements of the periodic table. The unusual nature of the carbon−carbon bond and the question concerning its bond order have attracted a lot of attention from theoretical chemists[69−72] in recent years. Around the equilibrium distance, the electronic structure of the C_2 molecule has two dominant configurations, $1\sigma_g^2 1\sigma_u^2 2\sigma_g^2 2\sigma_u^2 1\pi_u^4$ and $1\sigma_g^2 1\sigma_u^2 2\sigma_g^2 1\pi_u^4 3\sigma_g^2$, as well as a number of other configurations arising from low-lying excited states.[66,73−75] When the two carbon atoms are pulled apart, the molecular system becomes strongly multireference. However, even for stretched carbon−carbon distances, dynamical electron correlation effects remain non-negligible.[46,73,75] A reliable theoretical description of spectroscopic constants (bond lengths, potential energy well depths, and vibrational frequencies) thus requires a balanced treatment of all types of electron correlation effects[45,76] (static, nondynamic, and dynamic) along the dissociation pathway. Since highly accurate reference data for the spectroscopic constants of C_2 is available, it is an ideal candidate to test our AP1roG-LCC approach.

The upper part of Table 1 summarizes the spectroscopic constants of the C_2 molecule for different basis sets and quantum chemistry methods, including various dynamical correlation models based on an AP1roG reference function. As expected, AP1roG predicts too short equilibrium bond distances and too shallow potential well depths for all basis sets studied. If dynamical correlation is included *a posteriori* on top of the AP1roG reference function using perturbation theory, then spectroscopic constants improve only slightly compared to MRCI-SD reference data. Although AP1roG-PTa predicts equilibrium bond distances that are in perfect agreement with MRCI-SD, the potential well depth is overestimated and the

DOI: 10.1021/acs.jctc.5b00776
J. Chem. Theory Comput. 2015, 11, 5252−5261

differences with respect to MRCI-SD are even larger than for AP1roG without PTa correction. Furthermore, AP1roG-PTb does not improve potential well depths and vibrational frequencies compared to AP1roG when the basis set is enlarged from aug-cc-pVDZ to aug-cc-pVTZ. In contrast to the PTa and PTb models, an LCC correction on top of AP1roG including doubles and singles and doubles yields spectroscopic constants that are in very good agreement with MRCI-SD reference data, outperforming NEVPT2 (differences are less than 2 kcal/mol for potential well depths using aug-cc-pVTZ).

Figure 1 shows the fitted potential energy surfaces for the aug-cc-pVTZ basis set. We should note that all potential energy surfaces were shifted to zero in the dissociation limit. Additional plots of all potential energy surfaces aligned at the equilibrium distance are summarized in Figures S1−S3 of the Supporting Information. Comparing the spectroscopic constants of Table 1, we can conclude that the MRCI-SD potential energy surface would lie between the AP1roG-LCCD and AP1roG-LCCSD potential energy curves. All other quantum chemistry methods yield potential energy surfaces that deviate more from the expected MRCI-SD reference curve.

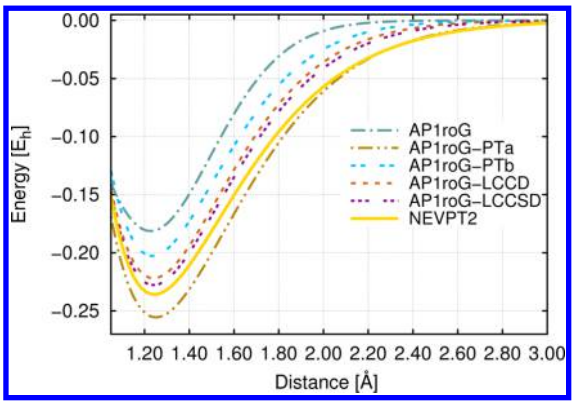

Figure 1. Potential energy surfaces for the dissociation of the C_2 molecule using the aug-cc-pVTZ basis set. See Figure S2 of the Supporting Information for potential energy surfaces aligned at the equilibrium distance.

4.2. Dissociation of F_2. F_2 is a well-known example of a diatomic molecule in which dynamical electron correlation effects play a dominant role.[72] Furthermore, theoretical studies indicate that large basis sets and robust dynamical electron correlation models are required to reproduce the experimentally determined spectroscopic constants.[77−82] These features make the F_2 molecule a good test case to assess the reliability of the LCC correction on top of an AP1roG reference function.

The middle part of Table 1 summarizes the spectroscopic constants for the dissociation process of the F_2 molecule using different basis sets and dynamical correlation models. We should note that both CCSD(T) and AP1roG-PTb diverge in the dissociation limit and thus the potential energy well depths are not given in Table 1 (see, also, Figure 2). To obtain an estimate for D_e, we have taken the MRCI-SD results by Peterson and co-workers.[66] Note that the r_e and ω_e, as predicted by MRCI-SD, are in good agreement with CCSD(T) calculations.

As observed for the C_2 molecule, AP1roG considerably overestimates the equilibrium bond length and underestimates the potential energy depth, which can be attributed to the large fraction of dynamical correlation that cannot be captured by restricting the wave function to electron-pair states. Although AP1roG-PTa yields potential energy depths that are in very good agreement with MRCI-SD reference data, equilibrium bond lengths and vibrational frequencies deviate considerably from the MRCI-SD reference values. Specifically, when increasing the basis set from aug-cc-pVDZ to aug-cc-pVTZ, the predicted equilibrium bond length changes from being too short to being too long. In contrast to PTa, AP1roG-PTb results in equilibrium bond lengths and vibrational frequencies that are in perfect agreement with MRCI-SD reference data when the basis set is increased to triple-ζ quality, but it fails in the vicinity of dissociation. The LCC correction on top of AP1roG results in the most stable and robust dynamical correlation model, yielding similar results for increasing basis set sizes and outperforming CCSD. Specifically, equilibrium bond lengths and vibrational frequencies are in very good agreement with MRCI-SD reference data. However, potential energy well depths are considerably overestimated by AP1roG-LCC (around 12 kcal/mol with respect to MRCI-SD), which might be attributed to restricting the cluster operator to single and double excitations[77] (cf. CCSD overestimates D_e by more than 20−35 kcal/mol, depending on the basis set size). The differences in potential energy surfaces with respect to CCSD(T) reference data are summarized in Figure S4 and Table S1 of the Supporting Information.

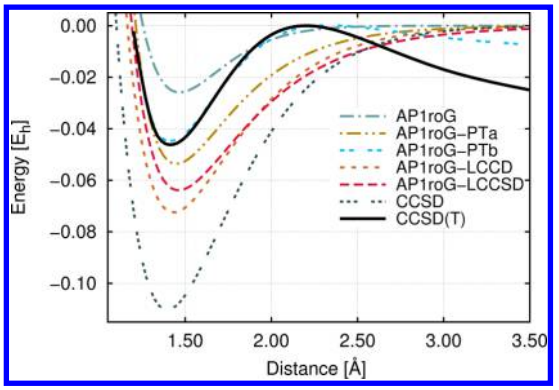

Figure 2. Potential energy surfaces for the dissociation of the F_2 molecule using the aug-cc-pVTZ basis set. See Figure S3 of the Supporting Information for potential energy surfaces aligned at the equilibrium distance.

4.3. Dissociation of BN. The BN molecule is isoelectronic to C_2 and has been intensely studied both experimentally and theoretically.[67,68,71,83−89] It represents a computationally challenging molecule, primarily because the lowest-lying electronic states possess strong multireference character. The ground state of the BN molecule has been confirmed (both experimentally and theoretically) to be the $^3\Pi$ state, which can be assigned the $1\sigma^2 2\sigma^2 3\sigma^2 4\sigma^2 1\pi^3 5\sigma$ electronic configuration, and is very close in energy to the lowest-lying $^1\Sigma^+$ state, which can be characterized by a $1\sigma^2 2\sigma^2 3\sigma^2 4\sigma^2 1\pi^4$ electronic configuration. Specifically, the $^1\Sigma^+$ excited state of BN dissociates to $B(^2P) + N(^2D)$, which are higher in energy than the corresponding ground state atoms, $B(^2P) + N(^4S)$. Due to its strong multireference character, the first excited state of the BN molecule represents another good test case to assess the accuracy of AP1roG and the dynamical correlation models.

The bottom part of Table 1 summarizes the spectroscopic constants for the dissociation process of the $^1\Sigma^+$ state of the BN molecule using different basis sets and dynamical correlation models. We should note that AP1roG-PTb diverges in the

DOI: 10.1021/acs.jctc.5b00776
J. Chem. Theory Comput. 2015, 11, 5252−5261

dissociation limit (for $r_{BN} \geq 3.50$ Å onward, not shown in Figure 2) and thus D_e is not given in Table 1. To obtain an estimate for the potential energy well depth, we have taken the MRCI-SD+Q results (including a multireference analog of the Davidson correction) by Peterson.[67] Note that r_e and ω_e, as predicted by MRCI-SD+Q, are in good agreement with RMR CCSD(T) calculations by Li and Paldus.[68]

As observed for the C_2 and F_2 molecules, AP1roG considerably overestimates the equilibrium bond length and underestimates the potential energy depth. Including dynamical correlation effects *a posteriori* using either perturbation theory or the LCC correction improves the errors in spectroscopic constants. The largest deviations from MRCI-SD+Q reference data are found for D_e, which is overestimated by more than 16 kcal/mol. Furthermore, while AP1roG-PTa yields equilibrium bond lengths that are in very good agreement with MRCI-SD +Q, AP1roG-LCCD and AP1roG-LCCSD result in smaller errors for the potential well depth. Specifically, when increasing the basis set from cc-pVDZ to cc-pVTZ, r_e predicted by AP1roG-PTa changes from being too short to being overestimated. Similar trends are found for the F_2 molecule. In contrast to C_2 and F_2, AP1roG-PTb results in spectroscopic constants that deviate the most from MRCI-SD+Q. As observed for homonuclear diatomics, the LCC correction based on an AP1roG reference function results in the most stable and robust dynamical correlation model, yielding similar results for increasing basis set sizes and outperforming CCSD(T).

The potential energy surfaces for the dissociation pathway of the $^1\Sigma$ state of BN are shown in Figure 3. Specifically, AP1roG predicts a rather flat and elongated dissociation curve. The shape of the potential energy curve changes considerably when adding dynamical correlation effects *a posteriori*, predicting a steeper dissociation pathway. We should note that all of the dynamical correlation models investigated in this work yield similar potential energy surfaces (cf. Table 1).

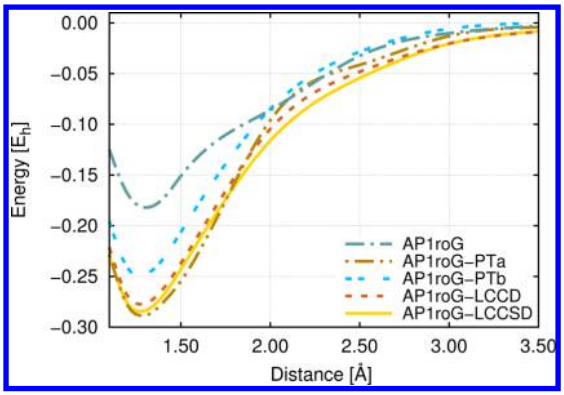

Figure 3. Potential energy surfaces for the dissociation of the first excited state of the BN molecule using the cc-pVTZ basis set. See Figure S3 of the Supporting Information for potential energy surfaces aligned at the equilibrium distance.

4.4. Symmetric Dissociation of H_{50}. The symmetric stretching of hydrogen chains is commonly used as a molecular model for strongly correlated systems and remains a challenging problem for conventional quantum-chemistry methods.[37,42,90−93] Recently, we have shown that AP1roG accurately describes the potential energy surface of the symmetric dissociation of H_{50} in the vicinity of dissociation, but it deviates from DMRG reference data around equilibrium and for stretched interatomic distances,[37] which can be attributed to the missing dynamical correlation energy.

Table 2 summarizes the nonparallelity error (NPE) per hydrogen atom for the symmetric dissociation of H_{50} obtained by AP1roG and different dynamical correlation models. The large NPE per hydrogen atom of AP1roG can be associated with the missing dynamical correlation energy around the equilibrium distance and for stretched interatomic bond lengths. Adding dynamical correlation *a posteriori* improves the NPE per hydrogen atom considerably. While PTa, PTb, and LCCD have a similar NPE per hydrogen atom of about 4.5 mE_h, the NPE is reduced to less than 1.5 mE_h if single excitations are included in the cluster operator.

Table 2. Nonparallelity Error per Hydrogen Atom for the Symmetric Dissociation of the H_{50} Chain with Respect to DMRG Reference Data[a]

method	NPE/H [mE_h]
MP2	43.540
AP1roG	6.187
AP1roG-PTa	4.831
AP1roG-PTb	4.170
AP1roG-LCCD	4.506
AP1roG-LCCSD	1.389

[a]The MP2 and AP1roG data are taken from ref 37.

The importance of single excitations in the LCC model is also noticeable in the shape of the potential energy surface shown in Figure 4. While AP1roG-PTa, AP1roG-PTb, and AP1roG-LCCD have similar potential energy curves (in terms of shape and total electronic energies), with AP1roG-PTb being lowest in energy, the potential energy surface obtained by AP1roG-LCCSD considerably deviates from the aforementioned dynamical correlation models for short and intermediate bond lengths (around 1.0 and 1.5 Å). Furthermore, the AP1roG-LCCSD potential energy curve is in very good agreement with DMRG reference data (Figure 4). The differences in potential energy surfaces with respect to DMRG reference data are summarized in Figure S5 and Table S2 of the Supporting Information.

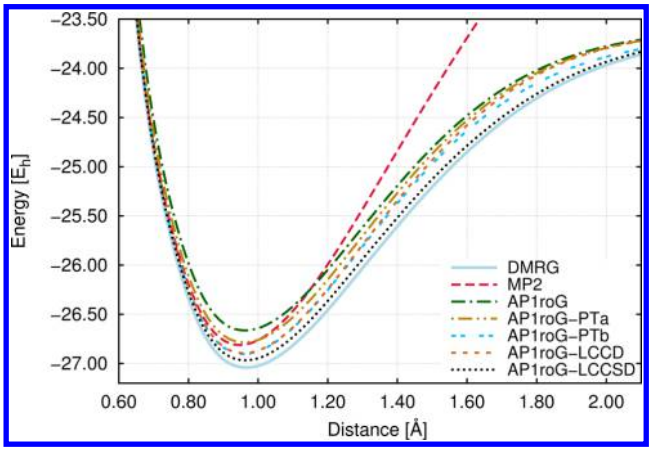

Figure 4. Symmetric dissociation of the H_{50} chain using the STO-6G basis set obtained from different methods. The DMRG reference data are taken from ref 90, whereas the MP2 and AP1roG data are taken from ref 37.

DOI: 10.1021/acs.jctc.5b00776
J. Chem. Theory Comput. 2015, 11, 5252−5261

4.5. Symmetric Dissociation of UO_2^{2+}. The uranyl cation (UO_2^{2+}) is a small building block of a large variety of uranium-containing complexes.[94−96] This molecule has a linear structure and a singlet ground-state electronic configuration. Its characteristic symmetric and asymmetric U−O vibrational frequencies are used to identify the presence of UO_2^{2+} in larger molecular assemblies.[95,97,98] While the electronic structure of the uranyl cation is well-understood around the equilibrium structure,[47,99−108] the complicated nature of the U−O bond hampers a theoretical description at larger U−O distances using standard quantum chemistry approaches.[47] One of the limiting factors that impede theoretical studies is the large number of strongly correlated electrons distributed among the 5f, 6d, and 7s orbitals. In addition, the 6s and 6p core−valence orbitals are easily polarizable and have a non-negligible contribution to the correlation energy. However, around the equilibrium structure, the uranyl cation is well-described by single-reference CC theory if all important electrons are correlated. This allows us to assess the performance of the LCC models in describing dynamical correlation effects originating from the 5f, 6d, and 7s as well as the core−valence electrons.

The equilibrium bond lengths and symmetric vibrational frequencies obtained by different quantum chemistry methods are shown in Table 3. As expected, AP1roG considerably underestimates the equilibrium bond length, whereas ω_e is in good agreement with CCSD(T). Adding dynamical correlation effects on top of AP1roG shifts r_e closer to the CCSD(T) reference data. The shape of the potential, however, strongly depends on the AP1roG dynamical correlation model. Specifically, PTb results in a much steeper potential energy surface, overestimating vibrational frequencies by more than 330 cm^{-1} compared to that with CCSD(T), whereas LCCD and LCCSD preserve the shape of the potential energy surface and yield a vibrational frequency that agrees well with AP1roG and CCSD(T) data (differences amount to approximately 20 cm^{-1}). The overall accuracy of AP1roG-LCC lies between those of CCSD and CCSD(T), being closer to the latter. We should emphasize that PTa completely fails for the UO_2^{2+} molecule and produces a discontinuous potential energy surface around equilibrium (Figure 5). Furthermore, the CASSCF equilibrium distance strongly depends on the size of the active space chosen in CASSCF calculations. Specifically, increasing the active space from CAS(10,10) to CAS(12,12), i.e., including the σ and σ^* orbitals, results in spectroscopic constants that are in good agreement with AP1roG-LCCD and CCSD(T) data.

Table 3. Spectroscopic Constants for the Symmetric Dissociation of the UO_2^{2+} Molecule for Different Quantum Chemistry Methods[a]

method	r_e [Å]	ω_e [cm^{-1}]
AP1roG	1.669(−0.047)	1062(+53)
AP1roG-PTb	1.715(−0.001)	1340(+331)
AP1roG-LCCD	1.712(−0.004)	997(−12)
AP1roG-LCCSD	1.724(+0.008)	1027(+18)
CAS(10,10)SCF	1.694(−0.022)	1079(+70)
CAS(12,12)SCF	1.707(−0.009)	1034(+25)
CCD	1.690(−0.026)	1125(+116)
CCSD	1.697(−0.019)	1068(+59)
CCSD(T)	1.716	1009

[a]The differences are with respect to CCSD(T) reference data. The CASSCF and CC data were taken from ref 47.

Figure 5 shows the fitted potential energy surfaces around equilibrium for selected quantum chemistry methods. AP1roG-LCC yields total electronic energies that are between those of CCSD and CCSD(T), whereas the potential energy surface predicted by AP1roG-PTb is considerably lower than the CCSD(T) reference curve. Note that the potential energy surfaces optimized by CASSCF lie much higher in energy and are thus not shown in Figure 5. The differences in potential energy surfaces with respect to CCSD(T) reference data are summarized in Figure S6 and Table S3 of the Supporting Information.

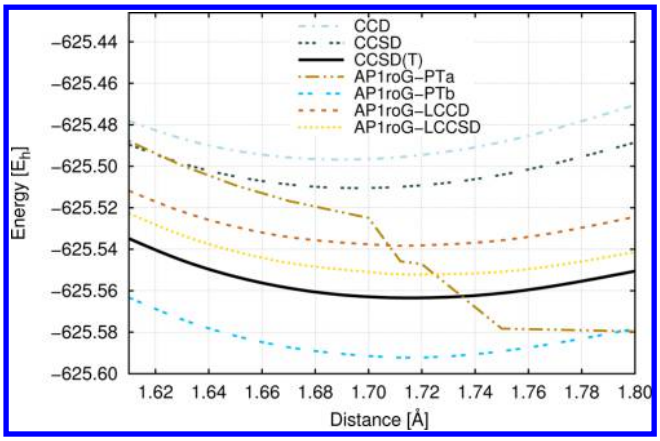

Figure 5. Potential energy surfaces for the symmetric stretching of the UO_2^{2+} molecule around the equilibrium geometry. Note that the CASSCF potential energy surfaces are much higher in energy and are thus not shown.

5. CONCLUSIONS

We have presented an alternative model to capture dynamical correlation effects on top of an AP1roG reference function that uses a linearized coupled cluster ansatz. Our approach is motivated by previous studies of an LCC correction to an APSG reference function.[55] Specifically, our cluster operator is restricted to double and single and double excitations as in the standard coupled cluster approach, i.e., excitations from the occupied to the virtual orbitals of some reference determinant. We have compared this new dynamical correlation ansatz to the PTa and PTb perturbation theory models as well as standard quantum chemistry approaches for the C_2 and F_2 molecules, the first excited state of the BN molecule, the H_{50} hydrogen chain, and the uranyl cation, UO_2^{2+}.

We should note that our LCC corrections are similar to fpCC methods, where the pair amplitudes are optimized first and then the equations for the remaining nonpair amplitudes are solved while the pair amplitudes are kept fixed. In contrast to fpCC, the cluster operator is linearized, and $|AP1roG\rangle$ is chosen as the reference function. This leads to additional terms in the amplitude equations, in contrast to the standard single-reference linearized CC approach, but fewer terms than in the fpCC method because of the missing higher-order terms of the nonpair amplitudes. The scaling of both LCC corrections is similar to CCD/CCSD, $O(o^2v^4)$ (o, occupied; v, virtual). Thus, AP1roG-LCC is computationally more expensive than

DOI: 10.1021/acs.jctc.5b00776
J. Chem. Theory Comput. 2015, 11, 5252−5261

AP1roG-PT, which scales as $O(K^5)$, where K is the number of basis functions.

In general, both AP1roG-LCC models yield similar spectroscopic constants and are closest to MRCI-SD, CCSD(T), and DMRG reference data for all molecules that we have investigated. Furthermore, LCCD and LCCSD represent more robust and reliable dynamical correlation models than PTa and PTb. Our study demonstrates that the success and failures of PTa and PTb are difficult to anticipate *a priori* and are strongly system-dependent. While PTa yields reasonable results for equilibrium bond lengths of the C_2 molecule and for the potential energy depth of the F_2 molecule, the corresponding C_2 potential energy depth and the F_2 equilibrium bond length significantly differ from reference data. A similar behavior was observed for PTb. In contrast to the perturbation theory models, the LCC ansatz is able to capture different flavors of dynamical correlation effects reliably, as present in the C_2, F_2, BN, H_{50}, and UO_2^{2+} molecules.

Furthermore, the LCC models presented in this work account for dynamical correlation effects *a posteriori*, i.e., the missing dynamical correlation effects that cannot be described by electron pairs. The orbital basis employed in the LCC corrections is, however, optimized using the AP1roG method and hence already includes a (small, but unknown) fraction of dynamical correlation effects. Adding dynamical correlation on top of AP1roG may thus lead to double counting of dynamical correlation effects. Moreover, our LCC models are equivalent to a MR-coupled electron pair approximation(0) (CEPA(0)) treatment, which is known to overestimate the electron correlation energy. Our laboratory is currently investigating the effect of orbital rotations, the extent of double counting, and the tendency to overestimate electron correlation.

Finally, we should emphasize that LCC is usually susceptible to divergences due to singularities in the amplitude equations, which can be redressed using regularization techniques.[109] For the molecules studied here, we did not encounter any problems with divergences when optimizing the LCC amplitudes. However, this might not be true for other systems. For example, the N_2 molecule is a particularly challenging system for electron-pair theories and *a posteriori* dynamical correlation models.[49,58] The performance of the LCC corrections and possible divergence problems in the LCC amplitude equations are currently being investigated in our laboratory and will be the subject of a future publication.

Nonetheless, our work suggest that AP1roG-LCC represents a computationally feasible and promising approach to account for dynamical correlation effects on top of AP1roG *a posteriori*. Further computational studies using a wider set of molecules are, however, required to scrutinize the performance and numerical stability of AP1roG-LCC.

■ ASSOCIATED CONTENT

Supporting Information

The Supporting Information is available free of charge on the ACS Publications website at DOI: 10.1021/acs.jctc.5b00776.

Potential energy surfaces for the dissociation of C_2 and F_2 molecules using the aug-cc-pVTZ basis set and for the singlet state of the BN molecule using a cc-pVTZ basis set; differences in potential energy surfaces with respect to CCSD(T) reference data for the dissociation of the F_2 molecule using the aug-cc-pVTZ basis set and with respect to DMRG reference data for the dissociation of the H_{50} molecule using the STO-6G basis set (PDF)

■ AUTHOR INFORMATION

Corresponding Author

*E-mail: katharina.boguslawski@gmail.com.

Funding

We gratefully acknowledge financial support from the Natural Sciences and Engineering Research Council of Canada. K.B. acknowledges financial support from the Swiss National Science Foundation (P2EZP2 148650), the Banting Postdoctoral Fellowship program, and the National Science Center (grant no. DEC-2013/11/B/ST4/00771).

Notes

The authors declare no competing financial interest.

■ ACKNOWLEDGMENTS

We had many helpful discussions with Paweł Tecmer and Ireneusz Grabowski.

■ REFERENCES

(1) Gagliardi, L.; Roos, B. *Nature* **2005**, *433*, 848−851.
(2) Jankowski, P.; McKellar, A.; Szalewicz, K. *Science* **2012**, *336*, 1147−1150.
(3) Rassolov, V. A. *J. Chem. Phys.* **2002**, *117*, 5978−5987.
(4) Surján, P. R.; Szabados, A.; Jeszenszki, P.; Zoboki, T. *J. Math. Chem.* **2012**, *50*, 534−551.
(5) Johnson, P. A.; Ayers, P. W.; Limacher, P. A.; De Baerdemacker, S.; Van Neck, D.; Bultinck, P. *Comput. Theor. Chem.* **2013**, *1003*, 101−113.
(6) Ellis, J. K.; Martin, R. L.; Scuseria, G. E. *J. Chem. Theory Comput.* **2013**, *9*, 2857−2869.
(7) Piris, M.; Ugalde, J. M. *Int. J. Quantum Chem.* **2014**, *114*, 1169−1175.
(8) Hurley, A. C.; Lennard-Jones, J.; Pople, J. A. *Proc. R. Soc. London, Ser. A* **1953**, *220*, 446−455.
(9) Parr, R. G.; Ellison, F. O.; Lykos, P. G. *J. Chem. Phys.* **1956**, *24*, 1106−1107.
(10) Parks, J. M.; Parr, R. G. *J. Chem. Phys.* **1958**, *28*, 335−345.
(11) Kutzelnigg, W. *J. Chem. Phys.* **1964**, *40*, 3640−2647.
(12) Kutzelnigg, W. *Theoret. Chim. Acta* **1965**, *3*, 241−253.
(13) Pernal, K. *Comput. Theor. Chem.* **2013**, *1003*, 127−129.
(14) Jeszenszki, P.; Rassolov, V.; Surján, P. R.; Szabados, Á. *Mol. Phys.* **2015**, *113*, 249−259.
(15) Coleman, A. J. *J. Math. Phys.* **1965**, *6*, 1425−1431.
(16) Coleman, A. J. *Int. J. Quantum Chem.* **1997**, *63*, 23−30.
(17) Neuscamman, E. *Phys. Rev. Lett.* **2012**, *109*, 203001.
(18) Neuscamman, E. *J. Chem. Phys.* **2013**, *139*, 194105.
(19) Jiménez-Hoyos, C. A.; Henderson, T. M.; Tsuchimochi, T.; Scuseria, G. E. *J. Chem. Phys.* **2012**, *136*, 164109.
(20) Bratoz, S.; Durand, P. *J. Chem. Phys.* **1965**, *43*, 2670−2679.
(21) Silver, D. M. *J. Chem. Phys.* **1969**, *50*, 5108−5116.
(22) Silver, D. M. *J. Chem. Phys.* **1970**, *52*, 299−303.
(23) Náray-Szabó, G. *J. Chem. Phys.* **1973**, *58*, 1775−1776.
(24) Náray-Szabó, G. *Int. J. Quantum Chem.* **1975**, *9*, 9−21.
(25) Surján, P. R. *Phys. Rev. A: At., Mol., Opt. Phys.* **1984**, *30*, 43−50.
(26) Surján, P. R.; Mayer, I.; Lukovits, I. *Phys. Rev. A: At., Mol., Opt. Phys.* **1985**, *32*, 748−755.
(27) Surján, P. R. *Int. J. Quantum Chem.* **1994**, *52*, 563−574.
(28) Surján, P. R. *Int. J. Quantum Chem.* **1995**, *55*, 109−116.
(29) Rosta, E.; Surján, P. R. *Int. J. Quantum Chem.* **2000**, *80*, 96−104.
(30) Surján, P. R. *Correlation and Localization*; Springer: Berlin, 1999; pp 63−88.
(31) Rosta, E.; Surján, P. R. *J. Chem. Phys.* **2002**, *116*, 878−889.
(32) Hay, P. J.; Hunt, W. J.; Goddard, W. A. *Chem. Phys. Lett.* **1972**, *13*, 30−35.

DOI: 10.1021/acs.jctc.5b00776
J. Chem. Theory Comput. 2015, 11, 5252−5261

(33) Goddard, W. A.; Dunning, T. H., Jr.; Hunt, W. J.; Hay, P. J. *Acc. Chem. Res.* **1973**, *6*, 368−376.
(34) Small, D. W.; Lawler, K. V.; Head-Gordon, M. *J. Chem. Theory Comput.* **2014**, *10*, 2027−2040.
(35) Lawler, K. V.; Beran, G. J. O.; Head-Gordon, M. *J. Chem. Phys.* **2008**, *128*, 024107.
(36) Limacher, P. A.; Ayers, P. W.; Johnson, P. A.; De Baerdemacker, S.; Van Neck, D.; Bultinck, P. *J. Chem. Theory Comput.* **2013**, *9*, 1394−1401.
(37) Boguslawski, K.; Tecmer, P.; Ayers, P. W.; Bultinck, P.; De Baerdemacker, S.; Van Neck, D. *Phys. Rev. B: Condens. Matter Mater. Phys.* **2014**, *89*, 201106.
(38) Stein, T.; Henderson, T. M.; Scuseria, G. E. *J. Chem. Phys.* **2014**, *140*, 214113.
(39) Weinhold, F.; Wilson, E. B. *J. Chem. Phys.* **1967**, *46*, 2752−2758.
(40) Henderson, T. M.; Dukelsky, J.; Scuseria, G. E.; Signoracci, A.; Duguet, T. *Phys. Rev. C: Nucl. Phys.* **2014**, *89*, 054305.
(41) Helgaker, T.; Jørgensen, P.; Olsen, J. *Molecular Electronic-Structure Theory*; Wiley: New York, 2000.
(42) Boguslawski, K.; Tecmer, P.; Limacher, P. A.; Johnson, P. A.; Ayers, P. W.; Bultinck, P.; De Baerdemacker, S.; Van Neck, D. *J. Chem. Phys.* **2014**, *140*, 214114.
(43) Boguslawski, K.; Tecmer, P.; Ayers, P. W.; Bultinck, P.; De Baerdemacker, S.; Van Neck, D. *J. Chem. Theory Comput.* **2014**, *10*, 4873−4882.
(44) Limacher, P. A.; Kim, T. D.; Ayers, P. W.; Johnson, P. A.; De Baerdemacker, S.; Van Neck, D.; Bultinck, P. *Mol. Phys.* **2014**, *112*, 853−862.
(45) Boguslawski, K.; Tecmer, P. *Int. J. Quantum Chem.* **2015**, *115*, 1289−1295.
(46) Tecmer, P.; Boguslawski, K.; Limacher, P. A.; Johnson, P. A.; Chan, M.; Verstraelen, T.; Ayers, P. W. *J. Phys. Chem. A* **2014**, *118*, 9058−9068.
(47) Tecmer, P.; Boguslawski, K.; Ayers, P. W. *Phys. Chem. Chem. Phys.* **2015**, *17*, 14427−14436.
(48) Rassolov, V. A.; Xu, F.; Garashchuk, S. *J. Chem. Phys.* **2004**, *120*, 10385−10394.
(49) Limacher, P.; Ayers, P.; Johnson, P.; De Baerdemacker, S.; Van Neck, D.; Bultinck, P. *Phys. Chem. Chem. Phys.* **2014**, *16*, 5061−5065.
(50) Jeszenszki, P.; Nagy, P. R.; Zoboki, T.; Szabados, Á; Surján, P. R. *Int. J. Quantum Chem.* **2014**, *114*, 1048−1052.
(51) Tóth, Z.; Nagy, P. R.; Jeszenszki, P.; Szabados, A. *Theor. Chem. Acc.* **2015**, *134*, 100.
(52) Pernal, K. *J. Chem. Theory Comput.* **2014**, *10*, 4332−4341.
(53) Pastorczak, E.; Pernal, K. *Phys. Chem. Chem. Phys.* **2015**, *17*, 8622−8626.
(54) Garza, A. J.; Bulik, I. W.; Alencar, A. G. S.; Sun, J.; Perdew, J. P.; Scuseria, G. E. *arXiv.org, e-Print Arch.* **2015**, arXiv:1509.03251.
(55) Zoboki, T.; Szabados, A.; Surjan, P. R. *J. Chem. Theory Comput.* **2013**, *9*, 2602−2608.
(56) Garza, A. J.; Bulik, I. W.; Henderson, T. M.; Scuseria, G. E. *J. Chem. Phys.* **2015**, *142*, 044109.
(57) Garza, A. J.; Bulik, I. W.; Henderson, T. M.; Scuseria, G. E. *Phys. Chem. Chem. Phys.* **2015**, *17*, 22412−22422.
(58) Henderson, T. M.; Bulik, I. W.; Stein, T.; Scuseria, G. E. *J. Chem. Phys.* **2014**, *141*, 244104.
(59) Kats, D.; Manby, F. R. *J. Chem. Phys.* **2013**, *139*, 021102.
(60) Kats, D. *J. Chem. Phys.* **2014**, *141*, 061101.
(61) Shavitt, I.; Bartlett, R. J. *Many-Body Methods in Chemistry and Physics: MBPT and Coupled-Cluster Theory*; Cambridge University Press: Cambridge, 2009.
(62) Verstraele, T.; Boguslawski, K.; Tecmer, P.; Heidar-Zadeh, F.; Chan, M.; Kim, T. D.; Zhao, Y.; Vandenbrande, S.; Yang, D.; González-Espinoza, C. E.; Limacher, P. A.; Berrocal, D.; Malek, A.; Ayers, P. W. *Horton 2.0.0*, 2015. http://theochem.github.com/horton/ .
(63) Aidas, K.; Angeli, C.; Bak, K. L.; Bakken, V.; Bast, R.; Boman, L.; Christiansen, O.; Cimiraglia, R.; Coriani, S.; Dahle, P.; et al. *WIREs Comput. Mol. Sci.* **2014**, *4*, 269−284.
(64) Coxon, J. A. *J. Mol. Spectrosc.* **1992**, *152*, 274−282.
(65) Abramowitz, M.; Stegun, I. A. *Handbook of Mathematical Functions with Formulas, Graphs, and Mathematical Tables*; Dover: New York, 1970.
(66) Peterson, K. A.; Kendall, R. A.; Dunning, T. H. *J. Chem. Phys.* **1993**, *99*, 9790−9805.
(67) Peterson, K. A. *J. Chem. Phys.* **1995**, *102*, 262−277.
(68) Li, X.; Paldus, J. *Chem. Phys. Lett.* **2006**, *431*, 179−184.
(69) Shaik, S.; Danovich, D.; Wu, W.; Su, P.; Rzepa, H. S.; Hiberty, P. C. *Nat. Chem.* **2012**, *4*, 195−200.
(70) Matxain, J. M.; Ruipérez, F.; Infante, I.; Lopez, X.; Ugalde, J. M.; Merino, G.; Piris, M. *J. Chem. Phys.* **2013**, *138*, 151102.
(71) Ramos-Cordoba, E.; Salvador, P.; Reiher, M. *Chem. - Eur. J.* **2013**, *19*, 15267−15275.
(72) Mottet, M.; Tecmer, P.; Boguslawski, K.; Legeza, Ö; Reiher, M. *Phys. Chem. Chem. Phys.* **2014**, *16*, 8872−8880.
(73) Abrams, M. L.; Sherrill, C. D. *J. Chem. Phys.* **2004**, *121*, 9211−9211.
(74) Jiménez-Hoyos, C. A.; Rodríguez-Guzmán, R.; Scuseria, G. E. *J. Chem. Phys.* **2013**, *139*, 224110.
(75) Wouters, S.; Poelmans, W.; Ayers, P. W.; Van Neck, D. *Comput. Phys. Commun.* **2014**, *185*, 1501−1514.
(76) Boguslawski, K.; Tecmer, P.; Legeza, Ö; Reiher, M. *J. Phys. Chem. Lett.* **2012**, *3*, 3129−3135.
(77) Jankowski, K.; Becherer, R.; Scharf, P.; Schiffer, H.; Ahlrichs, R. *J. Chem. Phys.* **1985**, *82*, 1413−1419.
(78) Ahlrichs, R.; Scharf, P.; Jankowski, K. *Chem. Phys.* **1985**, *98*, 381−386.
(79) Li, X.; Paldus, J. *J. Chem. Phys.* **1998**, *108*, 637−648.
(80) Kowalski, K.; Piecuch, P. *Chem. Phys. Lett.* **2001**, *344*, 165−175.
(81) Ivanov, V. V.; Adamowicz, L.; Lyakh, D. I. *Int. J. Quantum Chem.* **2006**, *106*, 2875−2880.
(82) Musiał, M.; Bartlett, R. J. *J. Chem. Phys.* **2005**, *122*, 224102.
(83) Mosher, O. A.; Frosch, R. P. *J. Chem. Phys.* **1970**, *52*, 5781−5783.
(84) Bredohl, H.; Dubois, I.; Houbrechts, Y.; Nzohabonayo, P. *J. Phys. B: At. Mol. Phys.* **1984**, *17*, 95−98.
(85) Bredohl, H.; Dubois, I.; Houbrechts, Y.; Nzohabonayo, P. *J. Mol. Spectrosc.* **1985**, *112*, 430−435.
(86) Karna, S. P.; Grein, F. *Chem. Phys.* **1985**, *98*, 207−219.
(87) Martin, J. M. L.; Lee, T. J.; Scuseria, G. E.; Taylor, P. R. *J. Chem. Phys.* **1992**, *97*, 6549−6556.
(88) Bauschlicher, C. W. J.; Partridge, H. *Chem. Phys. Lett.* **1996**, *257*, 601−608.
(89) Karton, A.; Martin, J. M. L. *J. Chem. Phys.* **2006**, *125*, 144313.
(90) Hachmann, J.; Cardoen, W.; Chan, G. K.-L. *J. Chem. Phys.* **2006**, *125*, 144101.
(91) Tsuchimochi, T.; Scuseria, G. E. *J. Chem. Phys.* **2009**, *131*, 121102.
(92) Stella, L.; Attaccalite, C.; Sorella, S.; Rubio, A. *Phys. Rev. B: Condens. Matter Mater. Phys.* **2011**, *84*, 245117.
(93) Lin, N.; Marianetti, C. A.; Millis, A. J.; Reichman, D. R. *Phys. Rev. Lett.* **2011**, *106*, 096402.
(94) Hayton, T. W. *Nat. Chem.* **2013**, *5*, 451−452.
(95) Denning, R. G. *J. Phys. Chem. A* **2007**, *111*, 4125−4143.
(96) Gomes, A. S. P.; Jacob, C. R.; Réal, F.; Visscher, L.; Vallet, V. *Phys. Chem. Chem. Phys.* **2013**, *15*, 15153−15162.
(97) Vallet, V.; Wahlgren, U.; Grenthe, I. *J. Phys. Chem. A* **2012**, *116*, 12373−12380.
(98) Tecmer, P.; Bast, R.; Ruud, K.; Visscher, L. *J. Phys. Chem. A* **2012**, *116*, 7397−7404.
(99) Denning, R. G. *Struct. Bonding (Berlin)* **1992**, *79*, 215−276.
(100) De Jong, W. A.; Visscher, L.; Nieuwpoort, W. C. *J. Mol. Struct.: THEOCHEM* **1998**, *458*, 41−52.
(101) Matsika, S.; Zhang, Z.; Brozell, S. R.; Blaudeau, J.-P.; Wang, Q.; Pitzer, R. M. *J. Phys. Chem. A* **2001**, *105*, 3825−3828.
(102) Réal, F.; Vallet, V.; Marian, C.; Wahlgren, U. *J. Chem. Phys.* **2007**, *127*, 214302.
(103) Pierloot, K.; van Besien, E. *J. Chem. Phys.* **2005**, *123*, 204309.

DOI: 10.1021/acs.jctc.5b00776
J. Chem. Theory Comput. 2015, 11, 5252−5261

(104) Jackson, V. E.; Craciun, R.; Dixon, D. A.; Peterson, K.; de Jong, W. B. *J. Phys. Chem. A* **2008**, *112*, 4095−4099.
(105) Réal, F.; Gomes, A. S. P.; Visscher, L.; Vallet, V.; Eliav, E. *J. Phys. Chem. A* **2009**, *113*, 12504−12511.
(106) Tecmer, P.; Gomes, A. S. P.; Ekström, U.; Visscher, L. *Phys. Chem. Chem. Phys.* **2011**, *13*, 6249−6259.
(107) Tecmer, P.; Govind, N.; Kowalski, K.; De Jong, W. A.; Visscher, L. *J. Chem. Phys.* **2013**, *139*, 034301.
(108) Tecmer, P.; Gomes, A. S. P.; Knecht, S.; Visscher, L. *J. Chem. Phys.* **2014**, *141*, 041107.
(109) Taube, A. G.; Bartlett, R. J. *J. Chem. Phys.* **2009**, *130*, 144112.

DOI: 10.1021/acs.jctc.5b00776
J. Chem. Theory Comput. 2015, 11, 5252−5261